Differential Detection with Intersymbol Interference and Frequency Uncertainty

JACK H. WINTERS, MEMBER, IEEE

Abstract—**In this paper we study differential detection of binary differential phase shift keyed (DPSK) signals with several impairments typical in satellite communication systems. In particular, the bit error rate is determined for bit timing error and frequency offset error at the receiver. The effect of a hard-limiting, band-limited repeater is also considered. The differential detector performance is determined for both conventional DPSK signals (with 0 and π phase shifts) and symmetrical DPSK signals (with $-\pi/2$ and $+\pi/2$ phase shifts). With symmetrical DPSK, adjacent bit signals are orthogonal rather than either in or out of phase. Therefore, with intersymbol interference, the error rates for all bits are equal and the average bit error rate is less with symmetrical DPSK, as shown in this paper.**

I. INTRODUCTION

DIFFERENTIAL phase shift keying (DPSK) with differential detection is often used in systems where carrier phase tracking is undesirable. In such systems, because the carrier phase is not tracked, carrier frequency uncertainty may be present at the receiver. Also, when bit timing is derived from the signal, there may be timing error at the receiver. Frequency and timing errors plus signal distortion caused by a repeater (when present) degrade the performance of the differential detector.

Previous studies have analyzed differential detection of the conventional binary DPSK signal (with 0 and 180° phase shifts with respect to the previous bit) with timing error [1], frequency offset [2], [3], and a repeater [4]-[7]. The effect of the intersymbol interference has been extensively analyzed (e.g., [8]-[11]), as has the effect of phase error (which is closely related to frequency offset) (e.g., [9], [12]). These studies were all primarily concerned with conventional binary DPSK. For conventional DPSK with intersymbol interference (caused by the repeater's filters or timing error at the receiver) the bit error probability is different for the data bits "0" and "1" because of the lack of symmetry of phase shifts for these bits, as noted in [1]. That is, with a 0° phase shift (for a "0"), intersymbol interference from adjacent bits will have no effect, while with a 180° phase shift (for a "1"), the effect will be maximum. The difference in bit error probabilities is undesirable and complicates the design of error correcting codes. However, except for [1], which deals with timing error only, the difference in the "0" and "1" data bit error probabilities due to intersymbol interference has not been previously studied.

A symmetrical form of binary DPSK uses ±90° phase shifts for data modulation [13, p. 340]. Since the signal is still binary DPSK, the bit error rate with differential detection is identical with that for conventional DPSK in the ideal case. However, with impairments the bit error rate for the two modulation techniques will differ. Because adjacent bit signal vectors are always orthogonal with the symmetrical modulation method, all bits have equal error rates. Furthermore, as shown in this paper, the average bit error rate is lower.

In this paper we analyze differential detection of conventional DPSK (with 0 and 180° phase shifts) and symmetrical DPSK (with ±90° phase shifts) with frequency offset and intersymbol interference at the receiver. We study the unequal error rates for "0" and "1" data bits with conventional DPSK and compare the results to symmetrical DPSK. The detector bit error rate is calculated assuming additive white Gaussian noise at the receiver. The sources of intersymbol interference considered are timing error and a hard-limited, band-limited repeater. Results show that with these impairments, the bit error rate is significantly lower with symmetrical DPSK.

In Section II we describe the modulation techniques and show how symmetrical DPSK can be implemented. The differential detector is described in Section III. A general equation for the bit error rate is given for differential detection with impairments. The error rate with frequency offset and timing error is studied in Section IV. In Section V we discuss the effect of a hard-limiting, band-limited repeater.

II. MODULATION TECHNIQUE

This section describes the conventional and symmetrical DPSK signals and discusses the implementation of the modulator for these signals. At the transmitter, the DPSK signal can be written as

$$S(t) = B \sin(\omega_0 t + \alpha(t)) \tag{1}$$

where B is an amplitude constant, ω_0 is the carrier radian frequency, and $\alpha(t)$ is the message carrying waveform. For the mth bit interval of duration T_b seconds (i.e., $(m-1)T_b < t \leq mT_b$), the message carrying waveform is given by

$$\alpha(t) = \alpha_m = \alpha_{m-1} + \pi/2\delta_m \tag{2}$$

where for conventional DPSK

$$\delta_m \triangleq \begin{cases} 0, & \text{when the } m\text{th data bit is a "0"} \\ 2, & \text{when the } m\text{th data bit is a "1"} \end{cases} \tag{3}$$

and for symmetrical DPSK

$$\delta_m \triangleq \begin{cases} -1, & \text{when the } m\text{th data bit is a "0"} \\ 1, & \text{when the } m\text{th data bit is a "1".} \end{cases} \tag{4}$$

Thus, for conventional DPSK the modulation scheme employed is the transmission of a "0" by a 0° phase shift and a "1" by a 180° phase shift, with respect to the preceding bit interval. For symmetrical DPSK, transmission of a "0" is

Paper approved by the Editor for Communication Theory of the IEEE Communications Society for publication without oral presentation. Manuscript received June 3, 1982; revised May 17, 1983. This work was supported in part by the Rome Air Development Center and The Ohio State University Research Foundation under Contract F30602-75-C-0061.

The author is with AT&T Bell Laboratories, Holmdel, NJ 07733.

0090-6778/84/0100-0025$01.00

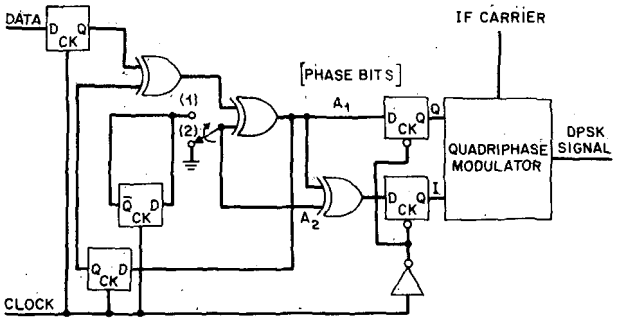

QUADRIPHASE MODULATOR LOGIC

PHASE BITS A_1	PHASE BITS A_2	I	Q	OUTPUT PHASE
0	0	0	0	270°
0	1	1	0	0°
1	0	1	1	90°
1	1	0	1	180°

Fig. 1. Schematic of the DPSK signal generation circuitry. The switch position determines whether symmetrical or conventional DPSK signals are generated.

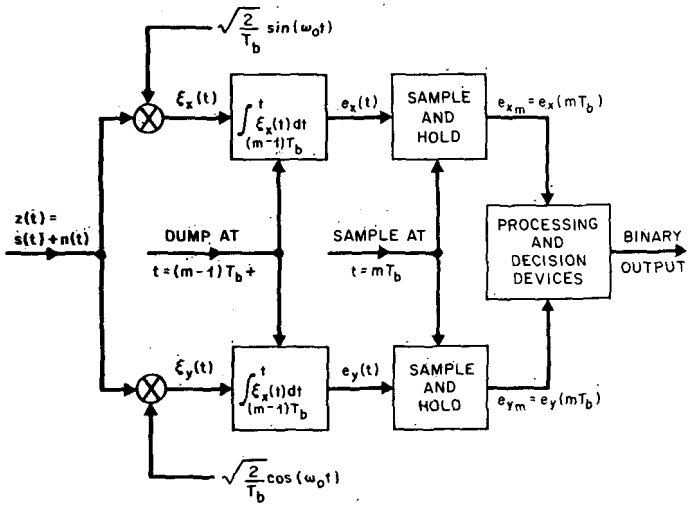

Fig. 2. The differential detector analyzed in this paper. The detector is the optimum M-ary DPSK receiver.

achieved by a -90° phase shift and a "1" by a 90° phase shift, with respect to the preceding bit interval.

Fig. 1 shows a way to implement the symmetrical DPSK modulation technique. When the switch is in position (1), a "1" data bit adds one (modulo 4) to the phase bits. (In Fig. 1, A_1 and A_2 are the most significant and least significant phase bits, respectively.) Similarly, a "0" data bit adds three to the phase bits. Logic changes the phase bits so that for each addition of one to these bits, the quadriphase modulator output is advanced by 90°, achieving the desired results. Note that the circuitry can easily be modified to generate conventional DPSK by setting A_2 to 0 [switch position (2)]. In this configuration the data bit "1" causes a 180° phase shift and a "0" no phase shift. Of course, only a biphase modulator is required in this case.

III. Differential Detection

This section presents a general discussion of the differential detector at the receiver. We first describe the differential detector studied in this paper and compare it to other differential detector types. A general formula is then presented for the detector bit error probability with additive white Gaussian noise.

Fig. 2 shows the differential detector analyzed in this paper. The received signal $z(t)$, consisting of the DPSK signal $s(t)$ and noise $n(t)$, is split into quadrature baseband components. These components are then integrated to generate the bit signal vector components. The mth bit signal vector is, therefore, given by

$$\bar{z}_m = e_{x_m}\bar{a}_x + e_{y_m}\bar{a}_y \tag{5}$$

where $\bar{a}_x$ and $\bar{a}_y$ are unit vectors defining a rectangular coordinate frame,[1] and e_{x_m} and e_{y_m} are the coefficients of these vectors, as shown in Fig. 2. Thus, the phase of $\bar{z}_m$ is the arctangent of the ratio of the bit signal vector components. The processing and decision devices use these coefficients (i.e., the signal vector phase) to determine the data bits. The differential detectors for conventional and symmetrical DPSK differ only in the receiver rule implemented in the processing and decision devices. The receiver rules are described below. Note that the detector of Fig. 2 can be used for differential detection of any M-ary DPSK signal simply by changing the receiver rule.

We will first consider the receiver rule for differential detection of a conventional DPSK signal. In the decision circuitry the magnitude of the angle between $\bar{z}_{m-1}$ and $\bar{z}_m$ defined in the interval $[0, \pi)$, i.e., the phase difference, is compared with a decision angle to determine the received bit. For ideal differential detection with equiprobable "0's" and "1's" in the presence of white Gaussian noise, the decision angle is $\pi/2$ rad. Therefore, the decision device employs the sign of the dot product of the two vectors, and the receiver rule is

$$\bar{z}_{m-1}\cdot\bar{z}_m = e_{x_{(m-1)}}e_{x_m} + e_{y_{(m-1)}}e_{y_m} > 0 \quad \text{"0" transmitted} \tag{6}$$

and

$$e_{x_{(m-1)}}e_{x_m} + e_{y_{(m-1)}}e_{y_m} \leq 0 \quad \text{"1" transmitted.} \tag{7}$$

Next, we will consider the receiver rule for differential detection of a symmetrical DPSK signal. In the decision circuitry the angle between $\bar{z}_{m-1}$ and $\bar{z}_m$ defined in the interval $[-\pi, \pi)$ is compared with the decision angle to determine the received bit. For ideal differential detection with equiprobable "0's" and "1's" in the presence of white Gaussian noise this decision angle is 0 rad. Therefore, the decision device uses the sign of the vector cross product of the two vectors. The receiver rule is

$$e_{x_{(m-1)}}e_{y_m} - e_{y_{(m-1)}}e_{x_m} > 0, \quad \text{"1" transmitted} \tag{8}$$

and

$$e_{x_{(m-1)}}e_{y_m} - e_{y_{(m-1)}}e_{x_m} \leq 0, \quad \text{"0" transmitted.} \tag{9}$$

The differential detector shown in Fig. 2 is of the same form as that shown in [14, p. 246]. As noted in [14], when the channel phase characteristic is constant for $2T_b$ seconds, this receiver "can be shown to be the optimum *a posteriori* probability computing receiver of differentially encoded, equiprobable, equal energy signals." However, the differential detector is often of another form, i.e., that shown in Fig.

[1] Note that complex notation could be used, but it seems easier to visualize the effect of timing error and frequency offset with the signal vector concept.

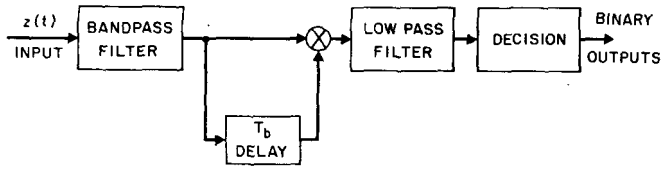

Fig. 3. A second possible implementation of the differential detector. This narrow-band IF-sampling detector is suboptimum because of intersymbol interference caused by the filters.

3. With this design, intersymbol interference and signal attenuation caused by the bandpass filter (which degrades the performance by at least 1.0 dB [15]) must be considered. However, because such filter effects have been neglected in most analyses, formulas derived for the detector of Fig. 3 can usually be used with the detector of Fig. 2. Therefore, in the analysis to follow we study the detector of Fig. 2, but also consider equations derived for the detector of Fig. 3.

From [13, p. 322] an equation can be obtained for the average bit error probability for differential detection with additive Gaussian noise. First, though, several definitions must be given. Let S_m be the mth bit received signal vector without noise. Then, we will define the mth bit received signal vector length as

$$L_m \triangleq |\bar{S}_m|. \tag{10}$$

The error in the phase shift at the mth bit (due, for example, to intersymbol interference or frequency error) will be defined as

$$\Delta\phi_e \triangleq \angle\bar{S}_m - \angle\bar{S}_{m-1} - \pi/2\delta_m. \tag{11}$$

Note that for ideal (i.e., no intersymbol interference or frequency uncertainty) differential detection,

$$L_m{}^2 = E_b \tag{12}$$

and

$$\Delta\phi_e = 0 \tag{13}$$

where E_b is the energy per bit. For given signal vectors and additive white Gaussian noise, the detector average bit error probability can now be determined (see Appendix A) to be given by

$$P_e = \frac{\gamma}{2\pi}\int_0^{\pi}\frac{e^{-(\alpha+\beta\cos\theta)}}{\alpha+\beta\cos\theta}\,d\theta \tag{14}$$

where

$$\gamma = \frac{L_1 L_2\cos(\Delta\phi_e)}{N_0} \tag{15}$$

$$\alpha = \frac{L_1{}^2 + L_2{}^2}{2N_0} \tag{16}$$

$$\beta = \sqrt{\alpha^2-\gamma^2} \tag{17}$$

and N_0 is the single-sided noise power spectral density. Equation (14) holds for

$$|\Delta\phi_e| < \frac{\pi}{2}. \tag{18}$$

Bit error probability equations that are numerically equivalent to (14) (although they are somewhat more complicated) are also given by [19, eq. (74)], [12, eq. (7)], and [8, eq. (22)].

With the above equations, the bit error rate with additive white Gaussian noise can be determined from the signal vectors without noise. Thus, in the following sections the signal vectors with each impairment are determined, and then the bit error rate with noise is computed.

IV. Frequency Offset and Timing Error Effects

To determine the signal vectors with frequency offset and timing error, we will make the following assumptions. First, the carrier frequency is assumed to be much greater than the data rate, i.e.,

$$\omega_0 \gg 2\pi/T_b. \tag{19}$$

Second, the phase shift per bit interval due to frequency offset at the receiver is assumed to be less than 90°, i.e.,

$$\Delta\omega T_b < \pi/2 \tag{20}$$

where $\Delta\omega$ is the difference in frequency between the received signal and the receiver local oscillator. Third, the frequency offset and bit timing error ϵ are assumed to vary slowly with respect to the data rate. The first assumption will, of course, hold in satellite communication systems. Because the bit error rate increases drastically as the phase shift per bit interval approaches 90°, the second assumption will also hold in most systems of interest. With respect to the third assumption, the dynamics of a satellite communication system allow only slow variations in $\Delta\omega$. Furthermore, in the typical case where bit timing is derived from the signal, timing error will, in general, change at a rate much less than the bit rate.

With the above assumptions, the signal vectors can be computed. For a given frequency offset and timing error magnitude less than one bit interval, the resultant signal vector for the $m-1$ bit can be calculated as (see Appendix B)

$$\begin{aligned}\bar{S}_{m-1} &= \sqrt{E_b}\left\{\frac{\sin(\Delta\omega T_b/2)}{(\Delta\omega T_b/2)}\left[\cos\left(\frac{\Delta\omega T_b}{2}+\alpha_{m-1}\right)\bar{a}_x + \sin\left(\frac{\Delta\omega T_b}{2}+\alpha_{m-1}\right)\bar{a}_y\right] - \frac{|\epsilon|}{T_b}\frac{\sin(\Delta\omega|\epsilon|/2)}{(\Delta\omega|\epsilon|/2)}\right.\\ &\cdot\left[\cos\left(\Delta\omega\left(\frac{T_b}{2}-\operatorname{sgn}(\epsilon)\left(\frac{T_b}{2}-\frac{|\epsilon|}{2}\right)\right)+\alpha_{m-1}\right)\bar{a}_x + \sin\left(\Delta\omega\left(\frac{T_b}{2}-\operatorname{sgn}(\epsilon)\left(\frac{T_b}{2}-\frac{|\epsilon|}{2}\right)\right)+\alpha_{m-1}\right)\bar{a}_y\right]\\ &+\frac{|\epsilon|}{T_b}\frac{\sin(\Delta\omega|\epsilon|/2)}{(\Delta\omega|\epsilon|/2)}\left[\cos\left(\Delta\omega\left(\frac{T_b}{2}-\operatorname{sgn}(\epsilon)\right.\right.\right.\\ &\cdot\left.\left.\left.\left(\frac{T_b}{2}-\frac{|\epsilon|}{2}\right)\right)+\alpha_{m-1}-\operatorname{sgn}(\epsilon)\frac{\pi}{2}\delta_a\right)\bar{a}_x\right.\\ &+\sin\left(\Delta\omega\left(\frac{T_b}{2}-\operatorname{sgn}(\epsilon)\left(\frac{T_b}{2}-\frac{|\epsilon|}{2}\right)\right)\right.\\ &\left.\left.+\alpha_{m-1}-\operatorname{sgn}(\epsilon)\frac{\pi}{2}\delta_a\right)\bar{a}_y\right]\Bigg\}\end{aligned} \tag{21}$$

where

$$\delta_a = \begin{cases} \delta_{m-1}, & \text{if } \epsilon \geq 0 \\ \delta_m, & \text{if } \epsilon < 0. \end{cases} \tag{22}$$

For $\bar{S}_m$, the vector equation is given by (21) with an increase in phase of $\Delta\omega T_b$, α_m substituted for α_{m-1}, and

$$\delta_a = \begin{cases} \delta_m, & \text{if } \epsilon \geq 0 \\ \delta_{m+1}, & \text{if } \epsilon < 0. \end{cases} \tag{23}$$

The above equations can be used with (10), (11), and (14) to determine the bit error rate with frequency offset and timing error.

Consider first the case of frequency offset only. In this case, for differential detection of conventional DPSK the bit error rate results given in [2] and [3] agree with those obtained using (14). It can also be shown that the bit error probability is the same for differential detection of both conventional and symmetrical DPSK with frequency offset (or with phase error [12]). It should also be noted that the bit error rate is independent of the data bits.

Consider next the case of timing error only. In this case, the bit error probability is dependent on the data bits. From (22) and (23), it can be seen that three data bits are needed to determine the average bit error rate from (14). Thus, there are eight (2^3) different bit combinations to consider. With symmetrical DPSK, adjacent bit signal vectors in the transmitted signal are always orthogonal. Therefore, the average bit error rate is the same for all bits. However, with conventional DPSK, if the bits are "0", adjacent bit signal vectors are identical, and, if the bits are "1", adjacent bits are 180° out of phase. Therefore, with timing error the bit error rate will be greater for a "1" than for a "0" (see Appendix C).

Fig. 4 illustrates the above points. In this figure, the bit error rate is plotted versus the energy per bit to noise density ratio with a timing error of 0.08 T_b. With conventional DPSK the average bit error rate for a "1" is seen to be several times greater than that for a "0". Furthermore, the average bit error rate for symmetrical DPSK is seen to be somewhat less than that for conventional DPSK. The improvement with symmetrical DPSK can be shown to increase with greater timing error.

The combined effect of frequency offset and timing error is shown in Fig. 5. The bit error rate is plotted versus timing error for several values of $\Delta\omega T_b$, with E_b/N_0 equal to 10. The results for conventional DPSK agree with the experimental results of [2]. For small frequency offset and timing error, symmetrical DPSK has a lower error rate than conventional DPSK because adjacent bit signals are approximately orthogonal rather than in or out of phase. As the frequency offset increases, however, the phase relationship between adjacent bit signals changes, and the advantage of symmetrical DPSK is reduced. For frequency offsets greater than $0.12\pi(\approx\pi/8)$, the relationships of the bit signal vectors are such [see (21)] that timing error increases the error rate of conventional DPSK to a lesser degree. Thus, it is interesting to note that, while the error rate for symmetrical DPSK is equal to or less than that for conventional DPSK with timing error or frequency offset alone, the error rate for symmetrical DPSK is higher with timing error and large frequency offsets. However, a 0.12π radian phase change per bit corresponds to a very large frequency offset. For example, with a 4 Mbit/s data rate, the frequency error must be greater than 1 MHz. Thus, in most systems, the error rate with symmetrical DPSK will be lower than with conventional DPSK.

At the receiver, bit timing is usually generated from the received signal. For example, bit timing can be obtained using a delay-lock loop (for coded signals), a digital-data-transition

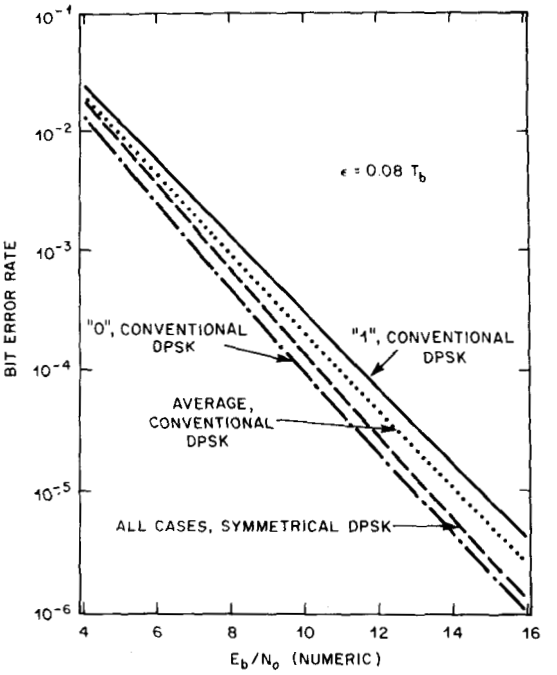

Fig. 4. Bit error rates for "0's" and "1's" for differential detection of conventional and symmetrical DPSK with timing error. The error rate is several times greater for a "1" as compared to a "0" with conventional DPSK, but is equal for both bits with symmetrical DPSK. Furthermore, the average error rate is less with symmetrical DPSK.

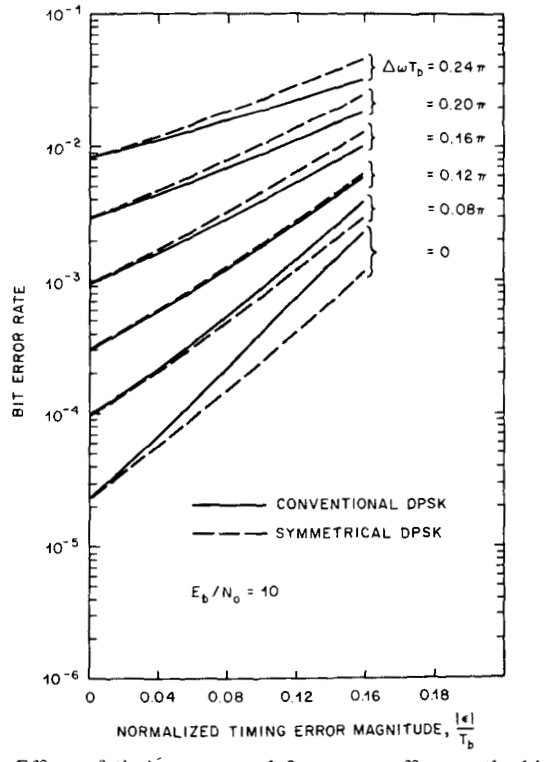

Fig. 5. Effect of timing error and frequency offset on the bit error rate. Conventional DPSK has a higher bit error rate than symmetrical DPSK except for large frequency offsets.

tracking loop, or an early-late gate bit synchronizer [14, ch. 9]. With these devices, the probability distribution of the timing error has been shown [20] to approach a Gaussian distribution for large signal-to-noise ratios. Thus, the average bit error rate is given by

$$P_e = \int_{\epsilon} P_e(\epsilon) p(\epsilon)\, d\epsilon \tag{24}$$

where $P_e(\epsilon)$ is the average bit error rate for a given timing error and

$$p(\epsilon) = \frac{1}{\sqrt{2\pi}\sigma_\epsilon} \exp\left[-\frac{(\epsilon - \bar{\epsilon})^2}{2\sigma_\epsilon{}^2}\right] \tag{25}$$

where $\bar{\epsilon}$ and σ_ϵ are the mean and standard deviation of the timing error, respectively.

As an example, the error rate will be determined when the bit timing is obtained with an absolute value bit synchronizer [14, ch. 9]. For conventional DPSK the standard deviation of the bit timing error is given by [14, eq. (9-79) with eq. (9-74), (9-75)]

$$\sigma_\epsilon = \left[\frac{W_L T_b}{8(E_b/N_0)\ \mathrm{erf}\left(\sqrt{\dfrac{E_b/N_0}{2}}\right)}\right]^{1/2} T_b \tag{26}$$

where W_L is the bit synchronizer filter bandwidth and erf(•) is the error function [21]. For symmetrical DPSK, the standard deviation is given by [19]

$$\sigma_\epsilon = \left(\frac{W_L T_b}{16(E_b/N_0)\ \mathrm{erf}\ (\sqrt{E_b/2N_0})}\right)^{1/2} T_b. \tag{27}$$

The error is less for symmetrical DPSK because phase shifts occur at every bit in the signal. In both cases the mean value of the timing error is zero.

Fig. 6 shows the effects of frequency offset when bit timing is generated with an absolute value bit synchronizer. In Fig. 6 the bit error is plotted versus E_b/N_0 for several values of frequency offset. Again the use of symmetrical DPSK is seen to reduce the bit error rate as compared to conventional DPSK. For example, with no frequency offset and E_b/N_0 equal to 16, the bit error rate with symmetrical DPSK is one-fifth that of conventional DPSK. Although the difference between the error rates with the two signals decreases with increasing frequency offset, symmetrical DPSK is better even for large frequency offsets.

V. Repeater Effects

This section considers the effect of a bandpass hard-limiting repeater on differential detection. The signal spectrum in the repeater is first considered, and then the bit error rate of the detector is studied.

Fig. 7 shows a block diagram of the system to be studied. The transmitted signal (without noise) is filtered, hard limited, filtered again, and retransmitted by the satellite repeater. At the receiver the received signal is corrupted by white Gaussian noise.[2] In the following discussion the bandpass filters considered are five pole Chebyshev filters with a maximum passband ripple of 0.05 dB.

[2] We assume the major noise contribution is due to the downlink noise.

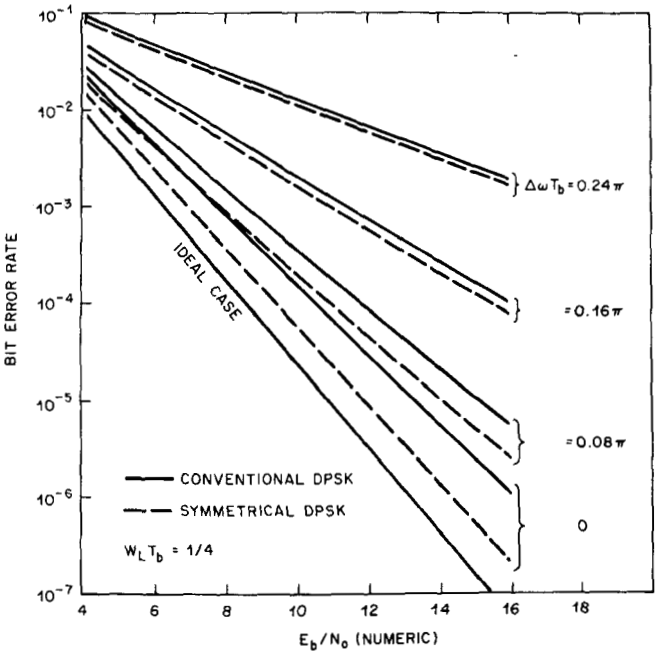

Fig. 6. The bit error rate with frequency offset and bit timing generated with an absolute value bit synchronizer. The error rate for symmetrical DPSK is significantly less than conventional DPSK for small frequency offsets.

The signal is modified in the repeater as shown in Figs. 8–13. Fig. 8 shows the power spectral density of a conventional DPSK signal with a 2.5 Mbit/s data rate. It can easily be shown that the spectra are identical for conventional and symmetrical DPSK signals. Thus, the spectra for the bandpass filtered signals, as shown in Fig. 9, are also the same. However, in the time domain the two signals are different, as shown in Figs. 10 and 11.

Because the phase transitions with symmetrical DPSK are only 90°, this signal when filtered has a more constant envelope. Thus, symmetrical DPSK is not as distorted by hard limiting, as shown in Figs. 12 and 13. The conventional DPSK spectrum sidelobes are regenerated, whereas the symmetrical DPSK spectrum is only slightly modified. As a result, when the hard-limited signal is filtered again, the symmetrical DPSK signal is less distorted.

Because the distortion is less with symmetrical DPSK, the error rate is lower at the detector. This is illustrated in Fig. 14. Here, the bit error rate is plotted versus E_b/N_0 for several values of repeater filter bandwidth to data rate ratios. The error rate was calculated by determining the signal vectors at the repeater output for all possible symbol sequences and using these values in (14). That is, the signal vectors were determined by integrating over each bit interval the time domain output of the filter-hard limiter simulator (typical simulator outputs are shown in Figs. 10 and 11). For each possible pair of signal vectors, the bit error rate with additive white Gaussian noise was determined using (14). The bit error rate values were then averaged to generate the results shown in Fig. 14. See [19] for further details.

Although the average error rate is only slightly lower with symmetrical DPSK, the error rate is the same for all bits. This is not true for conventional DPSK, as illustrated in Fig. 15.

VI. Summary and Conclusions

In this paper we have studied differential detection of binary DPSK signals with several impairments. The combined effect of frequency offset and timing error at the

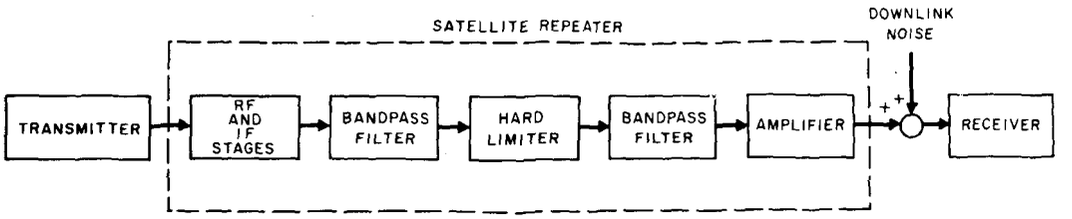

Fig. 7. Block diagram of the communication system with a repeater. The signal is distorted by the bandpass filters and hard limiter.

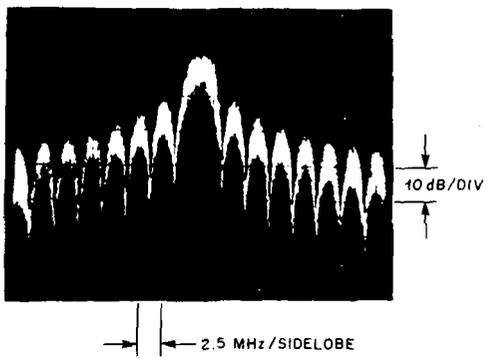

Fig. 8. The experimental DPSK signal power density spectrum (2.5 MHz data rate and pseudorandom input data). The spectrum is the same for both conventional and symmetrical DPSK.

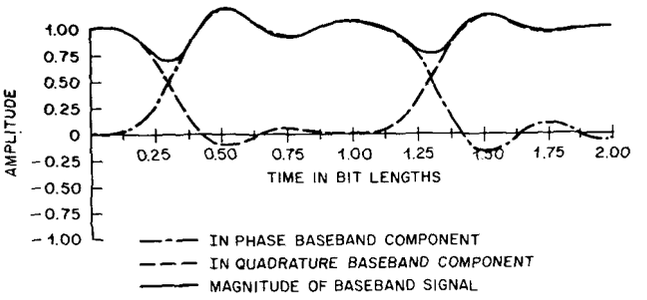

Fig. 11. Theoretical band-limited baseband symmetrical DPSK signal (periodic "0" – "1" input data bits and the same filter as used for Fig. 10). The signal exhibits a much smoother envelope than filtered conventional DPSK. Thus, the signal will be less distorted by a hard limiter.

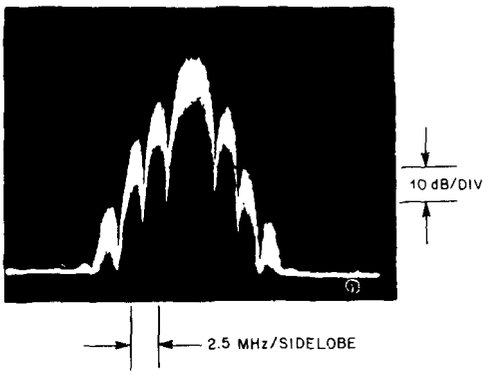

Fig. 9. The experimental band-limited DPSK signal power density spectrum (five-section, 10 MHz bandwidth Chebyshev filter with 0.05 dB peak-to-peak passband ripple). Again the spectrum is the same for symmetrical and conventional DPSK. However, in the time domain the two signals are completely different, as shown in Figs. 10 and 11.

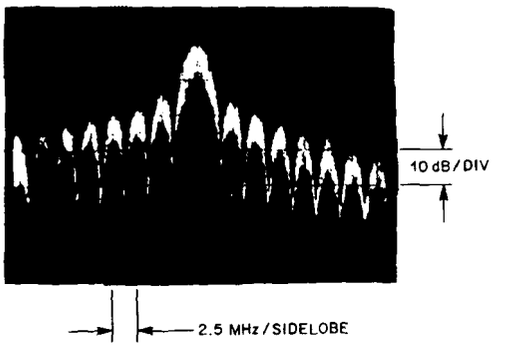

Fig. 12. The experimental band-limited conventional DPSK signal power density spectrum after hard limiting. The sidelobes have been regenerated and the spectrum is almost identical to that before filtering.

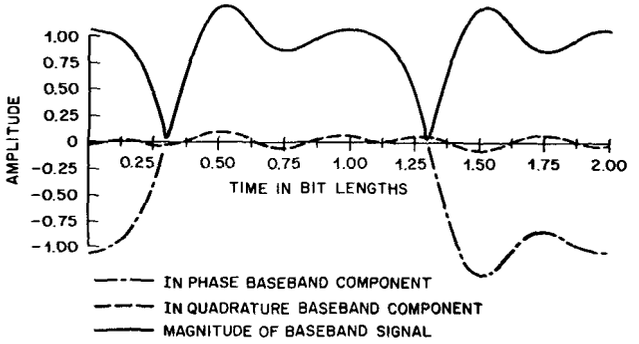

Fig. 10. Theoretical band-limited baseband conventional DPSK signal (all "1" data bits and five-section Chebyshev filter with a bandwidth of four times the data rate and 0.05 dB peak-to-peak passband ripple). There is a wide variation in signal envelope.

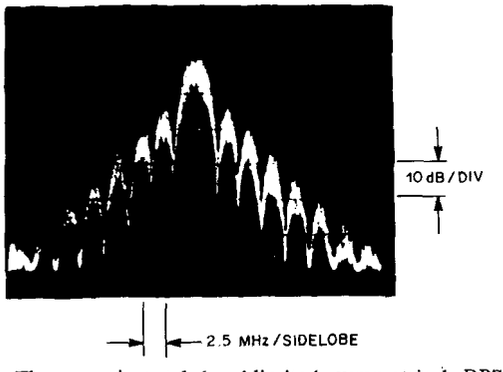

Fig. 13. The experimental band-limited symmetrical DPSK signal power density spectrum after hard limiting. Since the sidelobes of the spectrum are lower than with conventional DPSK, the symmetrical DPSK signal will be less distorted by a bandpass filter.

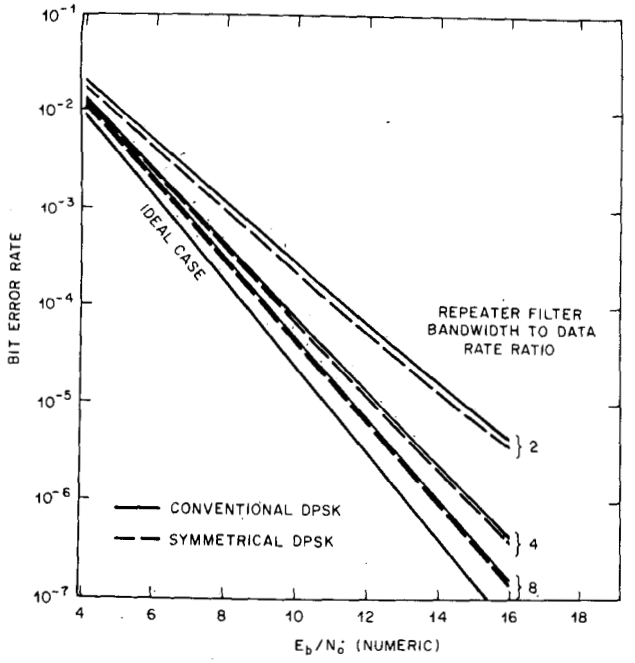

Fig. 14. Effect of repeater bandwidth on the average bit error rate. Symmetrical DPSK has a slightly lower error rate than conventional DPSK.

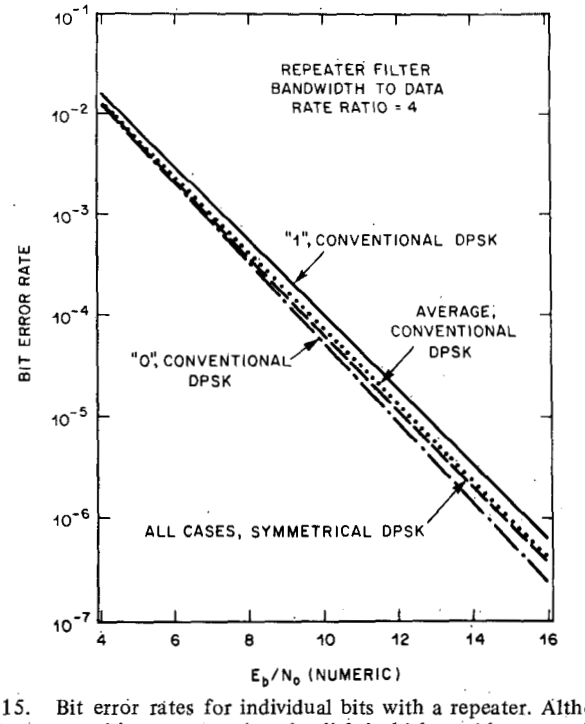

Fig. 15. Bit error rates for individual bits with a repeater. Although the average bit error rate is only slightly higher with conventional DPSK, there can be a large difference in the error rates for a "0" and a "1". With symmetrical DPSK, however, the error rate is the same for both bits.

receiver was studied, as was the effect of a hard-limiting, band-limited repeater.

Conventional DPSK with 0 and 180° phase shifts was compared to symmetrical DPSK with ±90° phase shifts. It was shown that symmetrical DPSK can be easily implemented and has the following advantages over conventional DPSK.

1) Lower average bit error rate for differential detection with timing error and frequency offset.

2) Less spectrum spreading when the band-limited signal is hard limited in a repeater. This results in a lower error rate at the receiver.

3) Equal error rates for all data bits. This is in contrast to conventional DPSK for which the error rate for a "1" can be several times higher than that for a "0" when intersymbol interference is present.

Appendix A

Derivation of the Bit Error Probability Equation

For differential detection of DPSK with additive white Gaussian noise, the bit error probability is given by (from [8, eq. (22)] as derived from [13, p. 322])[3]

$$P_e = \frac{\sigma_1^2}{\sigma_1^2+\sigma_2^2}\left[1 - Q\left(\frac{a_+}{\sqrt{\sigma_1^2+\sigma_2^2}}, \frac{a_-}{\sqrt{\sigma_1^2+\sigma_2^2}}\right)\right] + \frac{\sigma_2^2}{\sigma_1^2+\sigma_2^2} Q\left(\frac{a_-}{\sqrt{\sigma_1^2+\sigma_2^2}}, \frac{a_+}{\sqrt{\sigma_1^2+\sigma_2^2}}\right) \quad \text{(A1)}$$

where

$$\sigma_1^2 = \sigma_2^2 = \sigma^2/2, \quad \text{(A2)}$$

$$\sigma^2 = N_0/2, \quad \text{(A3)}$$

$$a_\pm = \left|\frac{L_1 \pm L_2 e^{j\Delta\phi_e}}{2}\right|, \quad \text{(A4)}$$

$Q(\cdot)$ is Marcum's Q function [16], and N_0 is the single-sided noise power spectral density. Thus, (A1) can be written as

$$P_e = \frac{1}{2}\left[1 - Q\left(\frac{a_+}{\sqrt{N_0/2}}, \frac{a_-}{\sqrt{N_0/2}}\right) + Q\left(\frac{a_-}{\sqrt{N_0/2}}, \frac{a_+}{\sqrt{N_0/2}}\right)\right] \quad \text{(A5)}$$

where

$$\frac{a_\pm}{\sqrt{N_0/2}} = \left(\frac{L_1^2 + L_2^2 \pm 2L_1L_2\cos\Delta\phi_e}{2N_0}\right)^{1/2}. \quad \text{(A6)}$$

Let

$$\alpha = \frac{L_1^2 + L_2^2}{2N_0} \quad \text{(A7)}$$

and

$$\gamma = \frac{L_1L_2\cos\Delta\phi_e}{N_0}. \quad \text{(A8)}$$

Then,

$$\frac{a_\pm}{\sqrt{N_0/2}} = (\alpha \pm \gamma)^{1/2}. \quad \text{(A9)}$$

[3] For notational convenience, we have set $m = 2$.

From (A6) and (A9),

$$P_e = \tfrac{1}{2}\left[1 - Q(\sqrt{\alpha+\gamma}, \sqrt{\alpha-\gamma}) + Q(\sqrt{\alpha-\gamma}, \sqrt{\alpha+\gamma})\right]. \quad \text{(A10)}$$

Now, it can be shown that

$$\sqrt{\alpha \pm \gamma} = \frac{\sqrt{\alpha+\beta} \pm \sqrt{\alpha-\beta}}{\sqrt{2}} \quad \text{(A11)}$$

where

$$\beta = \sqrt{\alpha^2 - \gamma^2}. \quad \text{(A12)}$$

Therefore, from [17, eq. (6-7)]

$$P_e = \frac{1}{2}\left[1 - \sqrt{1 - \left(\frac{\beta}{\alpha}\right)^2} I_e\left(\frac{\beta}{\alpha}, \alpha\right)\right] \quad \text{(A13)}$$

or

$$P_e = \frac{1}{2}\left[1 - \frac{\gamma}{\alpha} I_e\left(\frac{\beta}{\alpha}, \alpha\right)\right] \quad \text{(A14)}$$

where, from [18, eq. (A3-5)]

$$I_e\left(\frac{\beta}{\alpha}, \alpha\right) = \frac{\alpha}{(\alpha^2-\beta^2)^{1/2}} - \frac{\alpha}{\pi}\int_0^{\pi} \frac{e^{-\alpha-\beta\cos\theta}}{\alpha+\beta\cos\theta} d\theta. \quad \text{(A15)}$$

Thus, from (A14) and (A15)

$$P_e = \frac{\gamma}{2\pi}\int_0^{\pi} \frac{e^{-(\alpha+\beta\cos\theta)}}{(\alpha+\beta\cos\theta)}\, d\theta. \quad \text{(A16)}$$

APPENDIX B

DERIVATION OF THE SIGNAL VECTOR EQUATION

The $m-1$ bit signal vector without noise is given by [from (5)]

$$\bar{S}_{m-1} = S_{x_{m-1}}\bar{a}_x + S_{y_{m-1}}\bar{a}_y \quad \text{(B1)}$$

where

$$S_{x_{m-1}} = \int_{(m-2)T_b}^{(m-1)T_b} S(t)\sqrt{\frac{2}{T_b}} \sin \omega_0 t\, dt \quad \text{(B2)}$$

and

$$S_{y_{m-1}} = \int_{(m-2)T_b}^{(m-1)T_b} S(t)\sqrt{\frac{2}{T_b}} \cos \omega_0 t\, dt. \quad \text{(B3)}$$

With bit timing error ϵ and frequency offset $\Delta\omega$, the received signal is given by [from (1)]

$$S(t) = \sqrt{2P_r}\sin((\omega_0 + \Delta\omega)(t+\epsilon) + \alpha(t+\epsilon)) \quad \text{(B4)}$$

where P_r is the received signal power ($P_r = E_b/T_b$).

Let us first consider $S_{x_{m-1}}$ with $\epsilon \geq 0$. From (B2) and (B4)

$$S_{x_{m-1}} = \frac{2}{T_b}\sqrt{E_b}\int_{(m-2)T_b}^{(m-1)T_b} \sin((\omega_0+\Delta\omega)(t+\epsilon) + \alpha(t+\epsilon))\sin\omega_0 t\, dt. \quad \text{(B5)}$$

By dropping high frequency terms, (B5) can be written as

$$S_{x_{m-1}} = \frac{\sqrt{E_b}}{T_b}\int_{(m-2)T_b}^{(m-1)T_b} \cos((\omega_0+\Delta\omega)\epsilon + \Delta\omega t + \alpha(t+\epsilon))\, dt \quad \text{(B6)}$$

or, with the values of $\alpha(t)$,

$$S_{x_{m-1}} = \frac{\sqrt{E_b}}{T_b}\left[\int_{(m-2)T_b}^{(m-1)T_b} \cos((\omega_0+\Delta\omega)\epsilon + \Delta\omega t + \alpha_{m-1})\, dt - \int_{(m-2)T_b}^{(m-2)T_b+\epsilon} \cos((\omega_0+\Delta\omega)\epsilon + \Delta\omega t + \alpha_{m-1})\, dt + \int_{(m-2)T_b}^{(m-2)T_b+\epsilon} \cos\left((\omega_0+\Delta\omega)\epsilon + \Delta\omega t + \alpha_{m-1} - \frac{\pi}{2}\delta_{m-1}\right)\right] dt. \quad \text{(B7)}$$

It is useful to note that

$$\int_a^{a+b} \cos(ct)\, dt = \frac{2\sin(c(b/2))\cos(c(a+b/2))}{c} \quad \text{(B8)}$$

Furthermore, because we are only interested in relative phase, without loss of generality let

$$(\omega_0+\Delta\omega)\epsilon + \Delta\omega(m-2)T_b = 0. \quad \text{(B9)}$$

Therefore, from (B8) and (B9), (B7) can be written as

$$S_{x_{m-1}} = \sqrt{E_b}\left[\frac{\sin(\Delta\omega T_b/2)}{\Delta\omega T_b/2}\cos(\Delta\omega T_b/2 + \alpha_{m-1}) - \frac{\epsilon}{T_b}\frac{\sin\Delta\omega\epsilon/2}{\Delta\omega\epsilon/2}\cos(\Delta\omega\epsilon/2 + \alpha_{m-1}) + \frac{\epsilon}{T_b}\cdot\frac{\sin\Delta\omega\epsilon/2}{\Delta\omega\epsilon/2}\cos\left(\Delta\omega\epsilon/2 + \alpha_{m-1} - \frac{\pi}{2}\delta_{m-1}\right)\right]. \quad \text{(B10)}$$

By following the above procedure for $S_{y_{m-1}}$, it can easily be shown that

$$S_{y_{m-1}} = \sqrt{E_b}\left[\frac{\sin(\Delta\omega T_b/2)}{\Delta\omega T_b/2}\sin(\Delta\omega T_b/2 + \alpha_{m-1}) - \frac{\epsilon}{T_b}\frac{\sin\Delta\omega\epsilon/2}{\Delta\omega\epsilon/2}\sin(\Delta\omega\epsilon/2 + \alpha_{m-1}) + \frac{\epsilon}{T_b}\cdot\frac{\sin\Delta\omega\epsilon/2}{\Delta\omega\epsilon/2}\sin\left(\Delta\omega\epsilon/2 + \alpha_{m-1} - \frac{\pi}{2}\delta_{m-1}\right)\right]. \quad \text{(B11)}$$

TABLE I
BIT ERROR RATES FOR CONVENTIONAL DPSK WITH POSITIVE TIMING ERROR ($0 < \epsilon < T/2$)*

bit m−1	bit m	L_{m-1}	L_m	Bit Error Rate for bit m
0	0	$\sqrt{E_b}$	$\sqrt{E_b}$	$\frac{1}{2}\exp\left(-\frac{E_b}{N_0}\right)$
1	0	$\sqrt{E_b}(1-2\epsilon)$	$\sqrt{E_b}$	$C(\epsilon)$**
0	1	$\sqrt{E_b}$	$\sqrt{E_b}(1-2\epsilon)$	$C(\epsilon)$**
1	1	$\sqrt{E_b}(1-2\epsilon)$	$\sqrt{E_b}(1-2\epsilon)$	$\frac{1}{2}\exp\left(-\frac{E_b(1-2\epsilon)^2}{N_0}\right)$

* For $\epsilon \geq T/2$, intersymbol interference causes bit errors to occur even without noise, and therefore the case is not considered in this Appendix.

** $C(\epsilon)$ can be determined from (14). However, it is sufficient to note that interchanging the values of L_{m-1} and L_m does not change the bit error rate.

By repeating the above process for $\epsilon < 0$ and combining the results into one equation, we obtain (21).

APPENDIX C

UNEQUAL BIT ERROR RATES FOR "0" AND "1" DATA BITS FOR CONVENTIONAL DPSK WITH INTERSYMBOL INTERFERENCE

Consider intersymbol interference caused by timing error at the detector. For positive timing error, detection of the mth data bit is affected by the $(m-1)$th data bit. Thus, there are four different bit combinations to consider as shown in Table I. For each pair of bits the signal vector magnitudes can be determined directly for the detector of Fig. 2 [or at least from (21) and (10)]. Thus, from Table I, with equiprobable "0's" and "1's" the average probability of error with a "0" data bit is given by

$$P_0 = \frac{1}{2}\left(\frac{1}{2}\exp\left(-\frac{E_b}{N_0}\right) + C(\epsilon)\right) \tag{C1}$$

and the average probability of error with a "1" data bit is given by

$$P_1 = \frac{1}{2}\left(\frac{1}{2}\exp\left(-\frac{E_b(1-2\epsilon)^2}{N_0}\right) + C(\epsilon)\right). \tag{C2}$$

Thus, for $0 < \epsilon < T/2$,

$$P_1 > P_0. \tag{C3}$$

Similar results can be obtained for negative timing error.

ACKNOWLEDGMENT

The author would like to thank his graduate advisor, Dr. Huff, for his guidance, and an anonymous reviewer for suggesting the bit error probability equation given by (14).

REFERENCES

[1] R. J. Huff, "An investigation of time division multiple access space communications systems," Ph.D. dissertation, Ohio State Univ., Columbus, 1969.
[2] T. W. Miller, "Imperfect differential detection of a biphase modulated signal—An experimental and analytical study," ElectroSci. Lab., Dep. Elec. Eng., Ohio State Univ., Rep. 2738-5, prepared under Contr. F30602-69-C-0112 for Rome Air Develop. Center, Griffiss AFB, NY, Aug. 23, 1971.
[3] J. C. Henry, III, "DPSK versus FSK with frequency uncertainty," *IEEE Trans. Commun. Technol.*, vol. COM-18, pp. 814–817, Dec. 1970.
[4] A. Weinberg, "Effects of a hard limiting repeater on the performance of a DPSK data transmission system," *IEEE Trans. Commun.*, vol. COM-25, pp. 1128–1133, Oct. 1977.
[5] J. S. Lee, R. H. French, and Y. K. Hong, "Error performance of differentially coherent detection of binary DPSK data transmission on the hard-limiting satellite channel," *IEEE Trans. Inform. Theory*, vol. IT-27, pp. 489–497, July 1981.
[6] G. J. Marshall, "Problems of receiver-filter design for a digitally modulated carrier system," *J. Sci. Technol.*, vol. 38, no. 4, pp. 174–182, 1971.
[7] B. T. Tan and T. T. Tjhung, "On binary DPSK error rates due to noise and intersymbol interference," *IEEE Trans. Commun.*, vol. COM-31, pp. 463–466, Mar. 1983.
[8] V. K. Prabhu and J. Salz, "On the performance of phase-shift-keying systems," *Bell Syst. Tech. J.*, vol. 60, pp. 2307–2343, Dec. 1981.
[9] W. M. Hubbard, "The effect of intersymbol interference on error rate in binary differentially-coherent phase-shift-keyed systems," *Bell Syst. Tech. J.*, vol. 46, pp. 1149–1172, July–Aug. 1967.
[10] O. Shimbo, M. I. Celebiler, and R. J. Fang, "Performance analysis of DPSK systems in both thermal noise and intersymbol interference," *IEEE Trans. Commun. Technol.*, vol. COM-19, pp. 1179–1188, Dec. 1971.
[11] J. S. Lee and L. E. Miller, "On the binary communication systems in correlated Gaussian noise," *IEEE Trans. Commun.*, vol. COM-23, pp. 255–259, Feb. 1975.
[12] N. M. Blachman, "The effect of phase error on DPSK error probability," *IEEE Trans. Commun.*, vol. COM-29, pp. 364–365, Mar. 1981.
[13] M. Schwartz, W. R. Bennett, and S. Stein, *Communication Systems and Techniques*. New York: McGraw-Hill, 1966.
[14] W. C. Lindsey and M. K. Simon, *Telecommunication Systems Engineering*. Englewood Cliffs, NJ: Prentice-Hall, 1973.
[15] J. H. Park, Jr., "On binary DPSK detection," *IEEE Trans. Commun.*, vol. COM-26, pp. 484–486, Apr. 1978.
[16] J. Marcum, "A statistical theory of target detection by pulsed radar," Math Appendix, Rep. RM-753, Rand Corp., July 1, 1948; reprinted in *IRE Trans. Inform. Theory*, vol. IT-6, p. 145, Apr. 1960.
[17] J. H. Roberts, *Angle Modulation*. England: Peregrinus, 1977.
[18] S. O. Rice, "Statistical properties of a sine wave plus random noise," *Bell Syst. Tech. J.*, vol. 27, pp. 109–157, Jan. 1948.
[19] J. H. Winters, "On the performance of an imperfectly-implemented symmetrical differential detector," ElectroSci. Lab., Dep. Elec. Eng., Ohio State Univ., Rep. 710300-3, prepared under Contr. F30602-75-C-0061 for Rome Air Develop. Center, Griffiss AFB, NY, Aug. 1978.
[20] M. K. Simon, "Nonlinear analysis of an absolute value type of an early-late gate bit synchronizer," *IEEE Trans. Commun. Technol.*, vol. COM-18, pp. 589–596, Oct. 1970.
[21] M. R. Spiegel, *Mathematical Handbook*. New York: McGraw-Hill, 1968, p. 183.

★

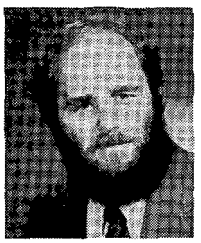

Jack H. Winters (S'77–S'78–S'80–M'82) was born in Canton, OH, on September 17, 1954. He received the B.S.E.E. degree from the University of Cincinnati, Cincinnati, OH, in 1977, and the M.Sc. and Ph.D. degrees in electrical engineering from The Ohio State University, Columbus, in 1978 and 1981, respectively.

From 1973 to 1976 he was a Professional Practice Student at the Communications Satellite Corporation, Washington, DC. He was a Graduate Research Associate with the ElectroScience Laboratory, The Ohio State University, from 1977 to 1981. Since 1981 he has been with the Radio Research Laboratory, AT&T Bell Laboratories, Holmdel, NJ, where he is studying digital satellite and mobile communication systems.

Dr. Winters is a member of Sigma Xi.